



Modeling left-truncated degradation data using random drift-diffusion Wiener processes

Bingxin Yan, Han Wang & Xiaobing Ma

To cite this article: Bingxin Yan, Han Wang & Xiaobing Ma (2023): Modeling left-truncated degradation data using random drift-diffusion Wiener processes, *Quality Technology & Quantitative Management*, DOI: [10.1080/16843703.2023.2187011](https://doi.org/10.1080/16843703.2023.2187011)

To link to this article: <https://doi.org/10.1080/16843703.2023.2187011>



[View supplementary material](#)



Published online: 15 Mar 2023.



[Submit your article to this journal](#)



Article views: 22



[View related articles](#)



CrossMark

[View Crossmark data](#)



Modeling left-truncated degradation data using random drift-diffusion Wiener processes

Bingxin Yan^a, Han Wang^b and Xiaobing Ma^a 

^aSchool of Reliability and Systems Engineering, Beihang University, Beijing, China; ^bSchool of Aeronautic Science and Engineering, Beihang University, Beijing, China

ABSTRACT

For products whose performance characteristic (PC) gradually degrades with time, one usually observes its degradation levels repeatedly to predict its remaining useful life (RUL). Due to the limited storage space of the server and the low resolution of a measurement instrument, we seldom record the low-magnitude degradation values at the early degradation stage in applications. Such observation setting introduces left-truncated degradation data, in which the data collection starts later than the unit's installation. This brings sampling biases and complicates the degradation data analysis. Moreover, due to the uncontrollable factors in applications, the degradation drift and the degradation diffusion may differ among various units. Motivated by an application of high-speed train bearings, we propose a Wiener process model for the left-truncated degradation data and jointly consider the drift-diffusion random effects. Closed-form formulas are available in the expectation-maximization (EM) algorithm for estimating the model parameters. We derive the RUL distribution in closed form. We also extend the proposed model to the multivariate degradation process. The parameters are estimated with the help of the Monte Carlo EM (MCEM) algorithm. An additional laser application illustrates the performance of the proposed model in RUL prediction, which may help to design a predictive maintenance strategy

ARTICLE HISTORY

Received 5 May 2022

Accepted 19 February 2023

KEYWORDS

Left-truncated degradation data; Wiener process; Random drift-diffusion; RUL prediction; Multivariate degradation

1 Introduction

1.1 Background

Degradation analysis is a useful tool for RUL prediction and predictive maintenance of products subject to degradation-induced failures (Bian et al., 2015) – (X. Liu et al., 2014). One usually collects the complete degradation data by monitoring the unit from a brand-new condition at its installation until failure. Proper modeling of the complete degradation data makes it able to predict the RUL accurately, which can provide the fundamental for predictive maintenance (Zhao et al., 2020) – (De Santis et al., 2022) and avoid safety issues (J. Lee et al., 2020). Generally speaking, three categories of method are suitable for degradation modeling: data-driven method (Su et al., 2020), model-based method (Singleton et al., 2016; Lu et al., 2020; Wang et al., 2018), and hybrid method (F. K. Wang & Mamo, 2019). Among them, the stochastic process has become mainstream over the years in the model-based method, including the Wiener process (Giorgio et al., 2020), Gamma process (Huynh, 2019)- (Tsai et al., 2011),

and Inverse Gaussian (IG) process (Ma et al., 2019). The Wiener process-based models, with ideal statistical properties and physical interpretations, show effective performance on the complete degradation data analysis (Shahraki et al., 2017).

Unfortunately, complete degradation data may be unavailable in engineering applications, such as the following three scenarios. First, when operators replace the measurement instrument, the degradation levels before the replacement may be missing (R. Zhou et al., 2012). Second, for highly reliable products, the degradation levels from the early degradation stage may be relatively low and unobservable, such as initial minor fatigue cracks on bearings. Third, if we conduct a burn-in test (or a robust test) (S. W. Liu et al., 2022) before selling the product to the customers, which subjects products to a harsh environment for a duration, degradation levels in the test would be unobservable for customers. Under all three scenarios, the data-collection process starts later than the installation of the unit, resulting in the left-truncated degradation data (Jiang et al., 2020; Wu et al., 2021). Examples of the truncated data include the light-emitting diode (LED) lumen degradation data (M. Y. Lee et al., 2017), wear paths of the hard disk drives (HDD) heads (Ye et al., 2015), and the degradation data of draught fans (Huynh, 2019). This brings sampling biases and makes degradation data analysis complicated.

On the other hand, it is a common observation that a higher degradation rate of the product would lead to higher degradation volatility (Ye & Xie, 2015). Such a correlation transfers the random effect in the degradation rate to the random effect in the degradation volatility. Examples include GaAs laser degradation data (Ye et al., 2015) and the LED accelerated degradation data (C. Y. Peng & Tseng, 2010) – (Zhai et al., 2018). All the above examples show positive correlations between degradation rate and degradation volatility, and the degradation rate and volatility vary among units. Therefore, the degradation rate-volatility correlation should be incorporated into the degradation model, and their random effects should be jointly considered. In this line, the Wiener process models usually link the drift and diffusion parameters with a positive function, thereby can jointly capture the random effects of degradation rate and volatility. One example is a new class of Wiener process models, which assumes $\sigma = \zeta v$ in the basic Wiener process model (Ye et al., 2015), where v and σ are the drift and diffusion parameters. Another example is the accelerated degradation model, which assumes that the drift and diffusion parameters increase with stress levels (C. Y. Peng & Tseng, 2010). As with the Wiener process, the parameters in the Gamma degradation process can also be linked to the stress level under an accelerated degradation test (Limon et al., 2020). However, the above examples and related works (Z. Wang et al., 2021) – (S. Zhou et al., 2021) are unsuitable for the left-truncated degradation data.

A motivating example of the left-truncated degradation data is the degradation data from the high-speed train rolling bearings. We collect the shock pulses from bearings under field conditions using an acceleration measurement instrument. In particular, two types of shock pulses that track the degradation of bearings are available. The first one is the decibel of the maximum shock value, denoted as dBsv, quantifying the strongest shock value during the measurement interval. The other is the normalized shock value, denoted as dBn, representing the educated shock pulse regardless of the working load on the bearing. For illustration, Figure 1 in Section 5.1 shows the extracted degradation features of four run-to-failure bearings (see more details about the data in Section 5.1). Ideally, the instrument should record the shock pulses from installation to the failure of the bearings. However, due to the server storage limitation and equipment measurement instrument replacement, the data during the early operating stage (with a low level of shock pulses) are missing, which leads to the left-truncated degradation data. Existing Wiener processes with the complete data assumption (Bian & Gebraeel, 2014b) might be inappropriate for the degradation modeling of the bearings. Moreover, for both dBsv and dBn, we fit each of the four bearings with a Wiener process model, i.e. $X(t) = vt + \sigma\mathcal{B}(\square)$ and obtain eight pairs of $(\hat{v}, \hat{\sigma}^2)$, which shows the randomness in both drift and diffusion parameters. Besides, linear regression analysis shows a strong positive correlation between the drift and diffusion parameters. This example motivates modeling left-truncated degradation data considering the drift-diffusion random effects.

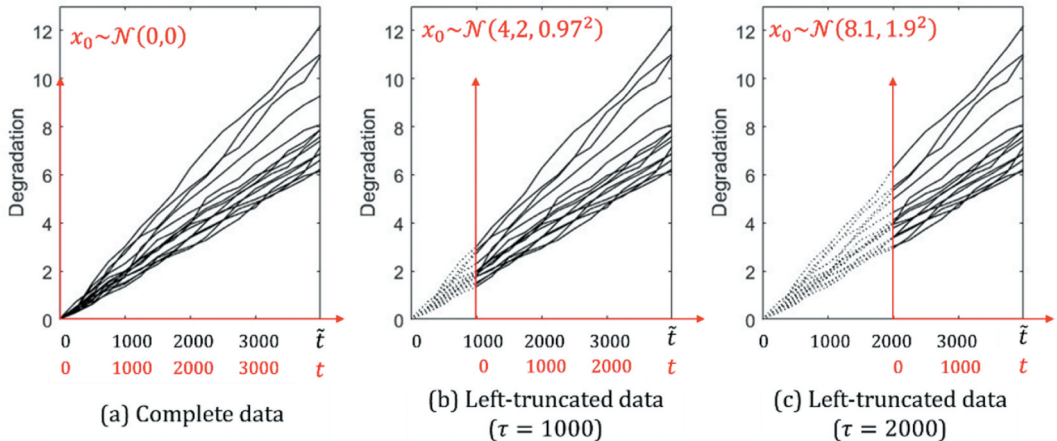


Figure 1. Examples of the complete and left-truncated degradation data. Here, \tilde{t} represents the calendar time and t represents the observation time.

Unlike the other widely studied factors (Neumann et al., 2019, X. Wang et al., 2020, Peng et al., 2019) in degradation modeling, i.e. the nonlinearity (J. X. Zhang et al., 2014), multi-source variability (Li et al., 2018), covariates (Z. Zhang et al., 2018), and multivariate degradation (Iscioğlu & Erem, 2021, Sun et al., 2020), few researchers concentrate on the randomness caused by the left-truncated degradation data. Existing works usually study the left-truncated degradation data from the perspective of random initiation. In this line, the initial degradation value x_0 observed at the truncation time τ is defined as initiation, and the initiation is imposed with a suitable distribution to make a traceable mathematical inference (Y. Zhang & Liao, 2014) – (Paroissin, 2015). Examples of suitable distribution include the normal distribution (Xiao & Ye, 2016) and the bivariate normal distribution (Weaver et al., 2013)– (Yuan & Pandey, 2009). These assumptions make the models fail to capture the time-variant property of the initiation. For illustration, we revisit the laser degradation data presented by Meeker et al (Meeker & Escobar, 2014). The complete degradation data, where the calendar time \tilde{t} is identical to the observation time t , are presented on the left of Figure 1 with zero initiation $x_0 = 0$. We truncate the complete data at calendar date $\tilde{t} = 1000$ and $\tilde{t} = 2000$, respectively, and the resulting truncated degradation data are presented in the middle and right of Figure 1, respectively. We fit the truncated degradation data using the Wiener process model with a normal initiation, $X(t) = x_0 + vt + \sigma B(t)$. The result in Figure 1 shows that both the mean and variance of the initiation change with the truncation time, which indicates a time-dependent random initiation for the left-truncated degradation data. Nevertheless, the current random initiation models, commonly assumed time-independent mean and variance of the initiation, fail to capture this dynamic. At present, only Shen et al (Shen et al., 2018) adopt the stochastic processes to describe time-dependent random initiation.

1.2 Overview

We aim to develop a Wiener process model for left-truncated degradation data and jointly consider the degradation drift-diffusion random effects. Contributions of this work are in three folds:

- (a) We provide a systematic framework on modeling, analysis, and prediction on the left-truncated degradation data. By considering the randomness of observation at the truncation time, we build a correlation between the initial observation and the degradation process.

- (b) We jointly consider the random effects of degradation drift and diffusion. By qualifying the correlation between degradation drift and diffusion with the nonlinear function, as practical experience suggests, we transfer the random effect in the drift parameter to the diffusion parameter.
- (c) Motivated by the bearing application, we extend the proposed model to multivariate degradation and provide methods on parameter estimation and RUL prediction.

The remainder of the paper is organized as follows. [Section 2](#) is the problem setup. [Section 3](#) proposes the random drift-diffusion Wiener process for left-truncated degradation data. The methods of parameter estimation and RUL prediction are provided. [Section 4](#) proposes the multivariate Wiener process model as a byproduct. In [Section 5](#), the performance of the proposed model is evaluated on lasers and bearings degradation data in univariate and multivariate degradation scenarios, respectively. Conclusions are drawn in [Section 6](#).

2 Problem setup

Considering a real-life engineering setting where the performance characteristic of the product gradually degrades with time, the product is assumed failure after the performance characteristic exceeds a threshold. The lifetime left before the product fails is concerned, referred to as the RUL. Before the product is sold to customers, manufacturers may want to develop a degradation test to assess the quality and reliability of the product. During the degradation test, they want to predict the RUL of the test unit at any possible time so that the test can be terminated timely to save the test cost. After the product is installed in the field, customers may want to predict the RUL of the product so that they can conduct predictive maintenance to avoid safety issues. Under both situations, the degradation observations may be left-truncated, where existing degradation modeling and RUL prediction methods are not applicable. Thus, a more sophisticated method is needed for both manufacturers and customers.

To formally describe our method, we describe the left-truncated observations first. Considering the product with a single degrading performance characteristic, the degradation level $X(\tilde{t})$ at calendar time \tilde{t} is observed under a left-truncated setting, as presented in [Figure 2](#). Specifically, the unit is installed at calendar time \tilde{t}_I , where the degradation of the unit starts, and it fails at calendar time \tilde{t}_L . The initial degradation level at \tilde{t}_I is $X(\tilde{t}_I) = \varphi$. We cannot observe the degradation levels from the very start of the degradation process, i.e. from calendar time \tilde{t}_I . As the calendar time comes to τ , we start observing the degradation levels. Here, τ is referred as the left-truncation time. We only consider the situation where the unit lifetime is longer than the truncation time, i.e.

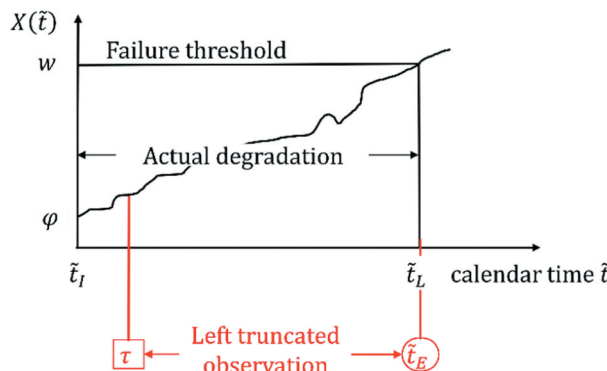


Figure 2. The left-truncated observations of a degradation process. The observation window in the calendar date is $[\tau, \tilde{t}_E]$. The installation happens at calendar time \tilde{t}_I . The failure happens at calendar time \tilde{t}_L .

$\tau < \tilde{t}_L - \tilde{t}_l$. Due to the randomness of degradation, the degradation level $X(\tilde{t} = \tau)$ at the beginning of the observation is a random variable. Without loss of generality, units in the same population are assumed under the same observation scheme, and thereby sharing the same left-truncation time τ . Besides, both the degradation drift and diffusion show heterogeneity among units.

3 Degradation modeling

3.1 Model construction

Consider the i th unit from a population of products. Let $X_i(t)$ denote the degradation process in observation time $t \geq 0$. We employ the Wiener process to model the left-truncated degradation data while jointly quantifying the random effects of degradation drift-diffusion. We introduce the truncation time τ to represent the time delay between the actual degradation of the product and the beginning of the observation. The Wiener process model for the observed degradation level for unit i is constructed as follows:

$$f(\Delta X_{ij}) = \frac{\sqrt{\beta}}{\pi\kappa\sqrt{\Delta t_{ij}}} \exp\left(\frac{\Delta X_{ij}}{\kappa^2} + \frac{\beta}{\alpha}\right) \sqrt{\frac{\mathcal{Z}_{ij}}{\mathcal{A}_{ij}}} \mathcal{K}_{-1}\left[\sqrt{\mathcal{A}_{ij}\mathcal{Z}_{ij}}\right] \quad (1)$$

where t is the observation time, $X_i(0) = \varphi + v_i\tau + \kappa\sqrt{v_i}B_i(\tau)$ is the initial observation at the truncation time τ , sharing the same Wiener process with the actual degradation process, φ is the initial value of the actual degradation, v_i is the drift parameter representing the degradation rate of unit i , $\kappa\sqrt{v_i}$ is the diffusion term representing the degradation volatility of unit i , the coefficient κ is common to all units $\{\text{unit}_i\}_{i=1}^n$ within the population, and $B_i(\cdot)$ is the standard Brownian motion of unit i .

To quantify the heterogeneities in a population, we introduce random effects in the proposed model in Equation 1 by letting v_i be a random variable following inverse Gaussian (IG) distribution, which is $v_i \sim \text{IG}(\alpha, \beta)$ with mean α and variance α^3/β . The widely used normal distribution may not apply in our case due to its negative support, as it is not compatible with the fact that $v_i > 0$. On the contrary, our assumption brings two advantages. On the one hand, the IG distribution has positive support, which is adapted to the actual situation. On the other hand, it accounts for the random effects in the degradation volatility, i.e. $\kappa^2 v_i \text{IG}(\kappa^2 \alpha, \kappa^2 \beta)$.

Our model shows superior properties compared to the basic Wiener process model. First, due to the consistency of the degradation mechanism over the whole life cycle, the model of the degradation process remains unchanged before and after the truncation time τ . Unlike existing models with Gaussian distributed initiation, we assume that the initial observation at the truncation time shares the same Wiener process with the observed degradation process, thereby capturing the homogeneity of the degradation process. Second, the proposed model can jointly describe the random effects of degradation drift and diffusion. Specifically, the drift parameter v_i can capture the randomness in degradation rates among different units, the diffusion term $\kappa\sqrt{v_i}$ can capture the randomness in degradation volatilities among units, and the standard Brownian motion $B_i(\cdot)$ can capture the randomness caused by unknown factors. Third, as reviewed in the introduction, the correlation between degradation rate and degradation volatility is a common observation according to most real-application data sets. Our model can readily capture such a correlation since both drift and diffusion terms share the same parameter v_i .

3.2 Parameter estimation

For the proposed model, the standard maximum likelihood estimation (MLE) is not qualified to estimate model parameters $\Theta = (\varphi, \alpha, \beta, \kappa, \tau)$ since no closed-form estimators can be obtained by directly maximizing the likelihood function. To solve this problem, the EM algorithm is adopted to

iteratively calculate the expectation of the likelihood function and then maximize the expectations. Denote $X_{ij} = X_i(t_{ij})$ as the observation of unit i at time t_{ij} , $i = 1, \dots, n, j = 1, \dots, m_i$. The degradation increments for unit i are denoted as $\Delta X_i = [\Delta X_{i1}, \dots, \Delta X_{im_i}]'$, where $\Delta X_{ij} = X_i(t_{ij}) - X_i(t_{ij-1})$ is the degradation increment from time t_{ij-1} to time t_{ij} . The observed degradation data are denoted as $X = \{\Delta X_{ij}, i = 1, \dots, n, j = 1, \dots, m_i\}$. Conditional on v , ΔX_{ij} follows a normal distribution $(\Delta X_{ij}|v) \tilde{\mathcal{N}}(v\Delta t_{ij}, \kappa^2 v\Delta t_{ij})$, where $\Delta t_{i1} = \tau + t_{i1}$ and $\Delta t_{ij} = t_{ij} - t_{ij-1}$, $j = 2, \dots, m_i$. The unconditional distribution of ΔX_{ij} is generally difficult to derive in closed forms. Fortunately, we solved this problem with the help of the second modified Bessel function. After integrating v out, the unconditional distribution of ΔX_{ij} is obtained as

$$f(\Delta X_{ij}) = \frac{\sqrt{\beta}}{\pi\kappa\sqrt{\Delta t_{ij}}} \exp\left(\frac{\Delta X_{ij}}{\kappa^2} + \frac{\beta}{\alpha}\right) \sqrt{\frac{\mathcal{Z}_{ij}}{\mathcal{A}_{ij}}} \mathcal{K}_{-1}\left[\sqrt{\mathcal{A}_{ij}\mathcal{Z}_{ij}}\right],$$

where

$$\mathcal{A}_{ij} = \frac{(\Delta X_{ij})^2}{\kappa^2 \Delta t_{ij}} + \beta,$$

$$\mathcal{Z}_{ij} = \frac{\beta}{\alpha^2} + \frac{\Delta t_{ij}}{\kappa^2},$$

and $\mathcal{K}_\alpha(z)$ is the second modified Bessel function given by

$$\mathcal{K}_a(z) = \frac{1}{2} \int_0^{+\infty} y^{a-1} \exp\left[-\frac{z}{2}\left(y + \frac{1}{y}\right)\right] dy.$$

The joint distribution of \mathbb{X} and v can be obtained by $f(\mathbb{X}|v) = \prod_{i=1}^n \prod_{j=1}^{m_i} f(\Delta X_{ij}|v) f(v)$. Again, by using the second modified Bessel function to integrate v out, we can obtain the unconditional joint distribution of the degradation increments \mathbb{X} as

$$f(\mathbb{X}) = \prod_{i=1}^n \prod_{j=1}^{m_i} \frac{\sqrt{\beta}}{\pi} \left(\frac{1}{\kappa\sqrt{2\pi}}\right)^{m_i} \frac{1}{\sqrt{\Delta t_{ij}}} \times \exp\left\{\frac{\beta}{\alpha} + \sum_{i=1}^n \frac{\Delta X_{i1} - \varphi}{\kappa^2} + \sum_{i=1}^n \sum_{j=2}^{m_i} \frac{\Delta X_{ij}}{\kappa^2}\right\} \\ \times \left(\frac{\mathcal{C}}{\mathcal{D}}\right)^{-\sum_{i=1}^n \frac{m_i+1}{4}} \mathcal{K}_{-\sum_{i=1}^n (m_i+1)/2}\left(\sqrt{\mathcal{CD}}\right),$$

where

$$\mathcal{C} = \beta + \sum_{i=1}^n \frac{(\Delta X_{i1} - \varphi)^2}{\kappa^2 \Delta t_{i1}} + \sum_{i=1}^n \sum_{j=2}^{m_i} \frac{(\Delta X_{ij})^2}{\kappa^2 \Delta t_{ij}} \quad (2)$$

$$\mathcal{D} = \frac{\beta}{\alpha^2} + \sum_{i=1}^n \frac{\Delta t_{i1}}{\kappa^2} + \sum_{i=1}^n \sum_{j=2}^{m_i} \frac{\Delta t_{ij}}{\kappa^2} \quad (3)$$

The log-likelihood function for degradation observations \mathbb{X} can be obtained by taking the logarithm of the joint distribution $f(\mathbb{X})$, which yields

$$\begin{aligned}\ell(\Theta|\mathbb{X}, v) = & \sum_{i=1}^n \left\{ \frac{1}{2} \ln \beta - \frac{1+m_i}{2} \ln 2\pi - \frac{3+m_i}{2} \ln v - \frac{\beta}{2\alpha^2} v - \frac{\beta}{2v} + \frac{\beta}{\alpha} \right\} \\ & + \sum_{i=1}^n \left\{ -m_i \ln \kappa - \frac{1}{2} \ln \Delta t_{i1} - \frac{1}{2} \sum_{j=2}^{m_i} \ln \Delta t_{ij} - \frac{(\Delta X_{i1} - \varphi)^2}{2\kappa^2 v \Delta t_{i1}} \right\} \\ & + \sum_{i=1}^n \left\{ -\frac{v \Delta t_{i1}}{2\kappa^2} + \frac{\Delta X_{i1} - \varphi}{\kappa^2} - \frac{1}{2\kappa^2 v} \sum_{j=2}^{m_i} \frac{(\Delta X_{ij})^2}{\Delta t_{ij}} - \frac{v}{2\kappa^2} \sum_{j=2}^{m_i} \Delta t_{ij} + \frac{1}{\kappa^2} \sum_{j=2}^{m_i} \Delta X_{i1} \right\}\end{aligned}$$

The EM algorithm, which iterates between E-step and M-step until a stopping criterion is achieved, is described as follows. Let $\Theta^{(l)}$ denote the estimates at the l -th iteration. In the E-step, we compute the expectation function $Q(\Theta|\Theta^{(l)}) = \mathbb{E}[\ln v(\Theta|\mathbb{X}, v)|\Theta^{(l)}]$ with respect to the drift parameter v . Before that, the conditional distribution of v given X is obtained based on the Bayesian formula, which can be written as

$$f(v|\mathbb{X}) = \frac{(\mathcal{D}/\mathcal{C})^{\frac{p}{2}}}{2\mathcal{K}_p(\sqrt{\mathcal{CD}})} v^{p-1} \exp\left\{-\frac{1}{2} (\mathcal{C}v^{-1} + \mathcal{D}v)\right\}. \quad (5)$$

By letting $p = -\sum_{i=1}^n (m_i + 1)/2$ and combining Equation 2 and Equation 3 into Equation 5. It is easy to find that $(v|\mathbb{X})$ follows a General Inverse Gaussian (GIG) distribution, i.e. $(v|\mathbb{X})\tilde{\mathcal{GIG}}(\mathcal{D}, \mathcal{C}, \sqrt{\cdot})$, which has the following expectations

$$\mathbb{E}[v|\mathbb{X}] = \frac{\mathcal{K}_{p+1}(\sqrt{\mathcal{CD}})}{\mathcal{K}_p(\sqrt{\mathcal{CD}})} \sqrt{\frac{\mathcal{C}}{\mathcal{D}}} \quad (6)$$

$$\mathbb{E}[v^{-1}|\mathbb{X}] = \frac{\mathcal{K}_{p-1}(\sqrt{\mathcal{CD}})}{\mathcal{K}_p(\sqrt{\mathcal{CD}})} \sqrt{\frac{\mathcal{D}}{\mathcal{C}}} \quad (7)$$

$$\mathbb{E}[\ln v|\mathbb{X}] = \sqrt{\mathcal{C}/\mathcal{D}}.$$

The expectation function $Q(\Theta|\Theta^{(l)})$ can be obtained by replacing v , v^{-1} and $\ln v$ with $\mathbb{E}[v|\mathbb{X}]$, $\mathbb{E}[v^{-1}|\mathbb{X}]$ and $\mathbb{E}[\ln v|\mathbb{X}]$ in Equation 4, which yields

$$\begin{aligned}Q(\Theta|\Theta^{(l)}) = & \sum_{i=1}^n \left\{ \frac{1}{2} \ln \beta - \frac{1+m_i}{2} \ln 2\pi - \frac{3+m_i}{2} [\ln v|\mathbb{X}] - \frac{\beta}{2\alpha^2} [v|\mathbb{X}] - \frac{\beta}{2} [v^{-1}|\mathbb{X}] \right\} \\ & + \sum_{i=1}^n \left\{ \frac{\beta}{\alpha} - m_i \ln \kappa - \frac{1}{2} \ln \Delta t_{i1} - \frac{1}{2} \sum_{j=2}^{m_i} \ln \Delta t_{ij} - \frac{(\Delta X_{i1} - \varphi)^2}{2\kappa^2 \Delta t_{i1}} [v^{-1}|\mathbb{X}] + \frac{\Delta X_{i1} - \varphi}{\kappa^2} \right\} \\ & + \sum_{i=1}^n \left\{ -\frac{\Delta t_{i1}}{2\kappa^2} [v|\mathbb{X}] - \frac{1}{2\kappa^2} \mathbb{E}[v^{-1}|\mathbb{X}] \sum_{j=2}^{m_i} \frac{(\Delta X_{ij})^2}{\Delta t_{ij}} - \frac{[v|\mathbb{X}]}{2\kappa^2} \sum_{j=2}^{m_i} \Delta t_{ij} + \frac{1}{\kappa^2} \sum_{j=2}^{m_i} \Delta X_{ij} \right\}\end{aligned}$$

In the M-step, by maximizing the expectation function $Q(\Theta|\Theta^{(l)})$ with respect to Θ , we can obtain the closed-form estimators for $\alpha^{(l+1)}$ and $\beta^{(l+1)}$ as

$$\alpha^{(l+1)} = \mathbb{E}[v|\mathbb{X}] \quad (8)$$

$$\beta^{(l+1)} = \frac{1}{\mathbb{E}[v^{-1}|\mathbb{X}] - 1/\alpha^{(l+1)}} \quad (9)$$

For estimating the parameters φ and κ , we can first obtain $\hat{\varphi}^{(l+1)}$ and $\hat{\kappa}^{(l+1)}$ as functions of parameter τ by maximizing the expectation function $Q(\Theta|\Theta^{(l)})$, which are given by

$$\hat{\varphi}^{(l+1)} = \frac{\mathbb{E}[v^{-1}|\mathbb{X}] \sum_{i=1}^n (\Delta X_{i1}/\Delta t_{i1}) - n}{\mathbb{E}[v^{-1}|\mathbb{X}] \sum_{i=1}^n (1/\Delta t_{i1})} \quad (10)$$

$$\begin{aligned} \left(\hat{\kappa}^{(l+1)}\right)^2 &= \left(\sum_{i=1}^n m_i\right)^{-1} \sum_{i=1}^n \left\{ \frac{(\Delta X_{i1} - \hat{\varphi}^{(l+1)})^2}{\Delta t_{i1}} \mathbb{E}[v^{-1}|\mathbb{X}] + \Delta t_{i1} \mathbb{E}[v|\mathbb{X}] - 2(\Delta X_{i1} - \hat{\varphi}^{(l+1)}) \right\} \\ &\quad + \left(\sum_{i=1}^n m_i\right)^{-1} \sum_{i=1}^n \left\{ \mathbb{E}[v^{-1}|\mathbb{X}] \sum_{j=2}^{m_i} \left[(\Delta X_{ij})^2 / \Delta t_{ij} \right] + \mathbb{E}[v|\mathbb{X}] \sum_{j=2}^{m_i} \Delta t_{ij} - 2 \sum_{j=2}^{m_i} \Delta X_{ij} \right\} \end{aligned}$$

The parameter $\tau^{(l+1)}$ can be estimated by maximizing the profile function

$$Q(\tau|\alpha^{(l+1)}, \beta^{(l+1)}, \hat{\varphi}^{(l+1)}, \hat{\kappa}^{(l+1)}) = - \sum_{i=1}^n \left\{ \frac{1}{2} \ln \Delta t_{i1} + \frac{(\Delta X_{i1} - \hat{\varphi})^2}{2(\hat{\kappa}^{(l+1)})^2 \Delta t_{i1}} \mathbb{E}[v^{-1}|\mathbb{X}] + \frac{\Delta t_{i1}}{2(\hat{\kappa}^{(l+1)})^2} \mathbb{E}[v|\mathbb{X}] \right\} \quad (12)$$

Due to the lack of the closed-form expression for the estimator $\tau^{(l+1)}$, numerical methods, such as the trust region algorithm, can be used to obtain $\tau^{(l+1)}$. After that, the estimators of parameters $\varphi^{(l+1)}$ and $\kappa^{(l+1)}$ can be obtained by substituting $\tau^{(l+1)}$ into Equation 10 and Equation 11. The algorithm iterates between the E-step and M-step until the estimates of the parameters converge. The details of the EM algorithm for the proposed model in Equation 1 are presented in Algorithm 1 in the Supplementary S.1.

For the computational complexity of the EM algorithm, the E-step has closed-form expectations of the random drift and is computed by iterating over all observations with computational complexity $\mathcal{O}(N)$, where $N = \sum_{i=1}^n m_i$ is the number of total observations. The M-step also has closed-form expressions for the estimators $\varphi^{(l)}$ and $\kappa^{(l)}$ at the l th step with computational complexity $\mathcal{O}(N)$. Moreover, the M-step also uses a numerical method to find the estimate $\tau^{(l)}$. As with Lu et al. [9], our simulation experience with the numerical algorithm shows that the average computing time increases linearly with the number of total observations. Therefore, the computational burden at each iteration of the EM algorithm is low.

We provide two practical guidelines for the EM algorithm for ease of implementation. First, an educated guess of the parameters ensures a fast implementation of the EM algorithm. We develop a workable procedure to find the educated guess, and the details are provided in Supplementary S.1. Second, a stopping threshold for the iterations is needed to ensure the high accuracy of the estimates. One commonly used way is to stop when the difference in estimate between two iterations is smaller than a threshold. The stopping threshold can be determined by plotting the estimates of the model parameters versus the number of iterations. We can also fix the number of iterations large enough to ensure the parameter estimates converge to a steady state.

3.3 RUL prediction

Based on the proposed model, we now derive the RUL distribution and conduct RUL prediction. Since the performance of a system degrades with usage, we define the RUL as the time interval between the current time and the first time when the degradation level exceeds the predetermined failure threshold w , which is $L_{ij} = \inf\{l_{ij} : X_i(t_{ij} + l_{ij}) \geq w | X_i(t_{ij}) < w\}$ for unit i at time t_{ij} . To

derive the RUL distribution, we first give the PDF of RUL condition on v , i.e. $(L_{ij}|v)\mathcal{IG}\left\{\left(\Xi - \mathcal{X}_{ij}\right)/v, \left(\Xi - \mathcal{X}_{ij}\right)^\epsilon/\kappa^\epsilon v\right\}$. By integrating v out, the unconditional distribution of the RUL L_{ij} can be derived as

$$f_{L_{ij}|X_{i,1j}}(l_{ij}) = \frac{\sqrt{\beta(w - X_{ij})}}{\pi\kappa\sqrt{l_{ij}^3}} \exp\left(\frac{w - X_{ij}}{\kappa^2} + \frac{\beta}{\alpha}\right) \sqrt{\frac{\mathcal{F}_{ij}}{\mathcal{E}_{ij}}} \mathcal{K}_{-1}(\mathcal{E}_{ij}\mathcal{F}_{ij}), \quad (13)$$

where

$$\mathcal{E}_{ij} = \frac{(w - X_{ij})^2}{\kappa^2 l_{ij}} + \beta,$$

$$\mathcal{F}_{ij} = \frac{l_{ij}}{\kappa^2} + \frac{\beta}{\alpha^2}.$$

Proof for Eq.(13): For the proposed model, based on the conditional distribution of RUL ($L_{ij}|v$) and the law of total probability, we have

$$f_{L_{ij}|\mathbf{X}_{1:n,1j}}(l) = \frac{\sqrt{\beta(w - X_{ij})^2}}{2\pi\kappa\sqrt{l_{ij}^3}} \int_0^{+\infty} \frac{1}{v^2} \exp\left\{-\frac{1}{2v}\left[\frac{(w - X_{ij})^2}{\kappa^2 v} + \beta\right] - \frac{v}{2}\left(\frac{l_{ij}}{\kappa^2} + \frac{\beta}{\alpha^2}\right) + \left(\frac{w - X_{ij}}{\kappa^2} + \frac{\beta}{\alpha}\right)\right\} dv \quad (14)$$

By substituting E_{ij} and F_{ij} into Equation 17, the unconditional distribution can be expressed as

$$f(l_{ij}) = \frac{\sqrt{\beta(w - X_{ij})^2}}{2\pi\kappa\sqrt{l_{ij}^3}} \exp\left\{\frac{w - X_{ij}}{\kappa^2} + \frac{\beta}{\alpha}\right\} \int_0^{+\infty} \frac{1}{v^2} \exp\left\{-\frac{\sqrt{\mathcal{E}_{ij}\mathcal{F}_{ij}}}{2}\left(\frac{1}{v}\sqrt{\frac{\mathcal{E}_{ij}}{\mathcal{F}_{ij}}} + v\sqrt{\frac{\mathcal{F}_{ij}}{\mathcal{E}_{ij}}}\right)\right\} dv$$

After replacing $v^{-1}\sqrt{\mathcal{E}_{ij}\mathcal{F}_{ij}}$ with y , the integration part in $f(l_{ij})$ can be expressed using the modified Bessel function of the second kind. Thus, the RUL distribution for the proposed model can be obtained, as shown in Equation 17. The quantiles and means of RUL can be readily obtained based on the PDF of RUL. ■

We also provide a procedure for practitioners to implement the proposed degradation modeling and RUL prediction method, as presented in Figure 3. The first step is to collect degradation levels

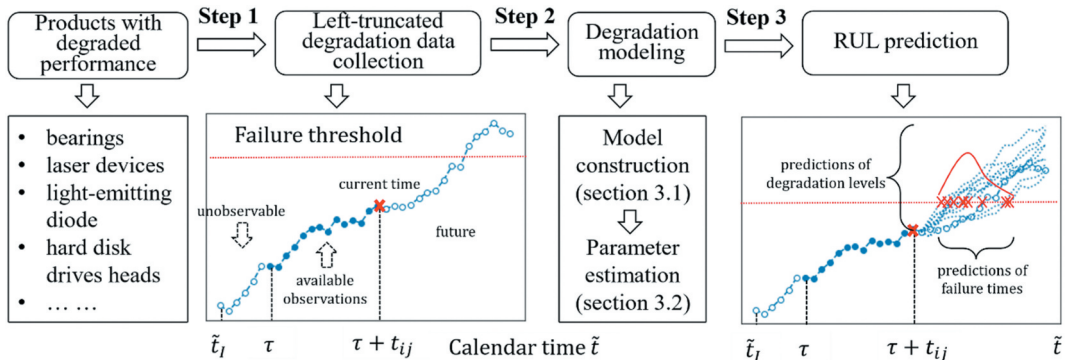


Figure 3. Implementation procedure of the proposed framework.

for the products with degraded performance characteristics. Given the left-truncated degradation data, practitioners can conduct degradation modeling in the second step following the methods in [Section 3.1](#) and [Section 3.2](#). Given the developed model, practitioners can predict the degradation levels and RUL in the third step following the method in this section.

4 Extension to multivariate degradation

If the product has only one PC, its degradation might be quite well modeled with the univariate Wiener process. Nevertheless, the degradation data have been fundamentally changed to the arrival of multivariate characteristics due to the advancement in sensor technology. Similarly, it is reasonable that all PCs will have left-truncated degradation observations and the jointly random effects of degradation drift and diffusion, such as the motivating example of bearings degradation in the introduction. This section extends the proposed model to multivariate degradation.

4.1 Model construction

Assume that unit i has d PCs degrading over time. Let $X_i(t) = [X_i^{(1)}(t), \dots, X_i^{(d)}(t)]'$ denote the multivariate degradation process in observation time $t \geq 0$, where $X_i^{(k)}(t)$ is the degradation process for the k th PC of unit i , $k = 1, \dots, d$, $i = 1, \dots, n$. By extending the proposed model in [Section 3.1](#), the degradation process for unit i is given by

$$X_i(t) = \varphi + v_i(\tau + t) + \sum_i^{1/2} \mathcal{B}_i(\tau + t), \quad (15)$$

where $X_i(0) = \varphi + v_i \tau + \sum_i^{1/2} \mathcal{B}_i(t)$, is the degradation level at the truncation time τ , sharing the same multivariate Wiener process with the degradation process. Here, $v_i = [v_{i1}, \dots, v_{id}]'$ is the vector of drift parameters and v_{ik} is the degradation rate of the k th PC, $\varphi = [\varphi_1, \dots, \varphi_d]'$ is the vector of initial degradation levels of d PCs at the beginning of the degradation process, and $\in R^{d \times d}$ is the covariance matrix. The diagonal elements of \in are $\kappa^2 v_{ik}$, $k = 1, \dots, d$, representing the degradation volatility of the k th PC, the off-diagonal elements of \in are zeros, and κ is a constant. Similarly, we introduce random effect in the degradation rate by letting $v_{ik} \sim \mathcal{IG}(\alpha_k, \beta_k)$. Here, α_k and β_k are the k th elements for $\alpha = [\alpha_1, \dots, \alpha_d]'$ and $\beta = [\beta_1, \dots, \beta_d]'$.

We offer two interpretations of the proposed model in terms of practical applications. First, it is not uncommon that the degradation level of one PC affects the degradation level of another PC from the same system ([Y. Zhang, 2022](#)). Without the extension to multivariate degradation, one would use the univariate degradation model in Equation 1 to independently model the degradation of multiple PCs. The incorrectly overlooking the correlation among multiple PCs would lead to biases in RUL predictions. The proposed model can capture such correlation through the covariance matrix in the multivariate Wiener process. Second, practitioners generally measure the degradation levels of multiple PCs in a system simultaneously due to economic considerations. Such an observation scheme leads to the same left-truncation time for the d PCs, which the proposed model also captures.

To formally describe the statistical inference, we provide several notations first. The degradation levels from d PCs of unit i at time t_{ij} are simultaneously measured and denoted as $X_{ij} = [X_{ij}^{(1)}, \dots, X_{ij}^{(d)}]'$, where $X_{ij}^{(k)}$ denotes the degradation measurement from the k th PC of unit i at time t_{ij} , $i = 1, \dots, n$, $j = 1, \dots, m_i$, $k = 1, \dots, d$. The degradation increment of unit i at time t_{ij} can be denoted as $\Delta X_{ij} = X_{ij} - X_{i,j-1}$. The vector of degradation increments $\Delta X_{ij} = [\Delta X_{ij}^{(1)}, \dots, \Delta X_{ij}^{(d)}]$ given v follows a multivariate normal distribution $\Delta X_{ij} \sim N\left(v \Delta t_{ij}, \sum^{1/2} \Delta t_{ij} \sum^{1/2}\right)$ with PDF

$$f(\Delta \mathbf{X}_{ij} | v) = (2\pi)^{-1/2} |\Sigma^{1/2} \Delta t_{ij} \Sigma^{1/2}|^{-1/2} \exp \left\{ -\frac{1}{2} (\Delta \mathbf{X}_{ij} - v \Delta t_{ij})' (\Sigma^{1/2} \Delta t_{ij} \Sigma^{1/2})^{-1} (\Delta \mathbf{X}_{ij} - v \Delta t_{ij}) \right\}.$$

The unit is defined failed when any of the degradation PCs exceeds its failure threshold w_k . The RUL is defined as $L_{ij} = \min\{L_{ijk}, k = 1, \dots, d\}$, where L_{ijk} represents the RUL of the k th PC, i.e. $L_{ijk} = \inf \left\{ l_{ijk} : X_i^{(k)}(t_{ijk} + l_{ijk}) \geq w_k | X_i^{(k)}(t_{ijk}) < w_k \right\}$.

4.2 Parameter estimation

Considering the proposed model in multivariate degradation, the EM algorithm is not qualified to estimate the model parameters since no closed-form expectations are available in the E-step. We develop an MCEM algorithm to estimate model parameters by using the Markov Chain Monte Carlo (MCMC) method in the E-step to approximate the expected log-likelihood function. Let $X = \{X_{ij} \in R^d, i = 1, \dots, n, j = 1, \dots, m_i\}$ denote the degradation data.

To develop the MCEM algorithm, the joint log-likelihood function based on degradation data X and random effects v can be decomposed into

$$\ell(\kappa, \alpha, \beta, \tau, \varphi | \mathbb{X}, v) = \ell_1(\kappa, \tau, \varphi | \mathbb{X}, v) + \ell_2(\alpha, \beta | v),$$

where

$$\ell_1(\kappa, \tau, \varphi | v, \mathbb{X}) = \sum_{i=1}^n \sum_{j=1}^{m_i} \left\{ -\frac{1}{2} \ln(2\pi |\Sigma \Delta t_{ij}|) - \frac{1}{2} (\Delta \mathbf{X}_{ij} - v \Delta t_{ij})' (\Sigma \Delta t_{ij})^{-1} (\Delta \mathbf{X}_{ij} - v \Delta t_{ij}) \right\},$$

and

$$\ell_2(\alpha, \beta | v) = \sum_{i=1}^n \sum_{j=1}^{m_i} \sum_{k=1}^d \left\{ \ln \alpha_k - \frac{1}{2} \ln(2\pi \beta_k v_k^3) - \frac{(v_k - \alpha_k)^2}{2v_k \beta_k} \right\},$$

where $\Delta t_{i1} = \tau + t_{i1}$, $\Delta X_{i1} = X_{i1} - \varphi$, and $\Delta X_{ij} = X_{ij} - X_{i,j-1}$, $\Delta t_{ij} = t_{ij} - t_{i,j-1}$ for $j = 2, \dots, m_i$.

Based on the description above, the MCEM algorithm can be provided now. Given the initial values for model parameters $\Theta^{(0)} = [\kappa^{(0)}, \alpha^{(0)}, \beta^{(0)}, \tau^{(0)}, \varphi^{(0)}]$, which can be obtained by independently fitting the degradation PCs to the proposed model in univariate degradation. The E-step focuses on obtaining the expectation of the joint log-likelihood function

$$Q(\Theta | \Theta^{(l)}) = \mathbb{E}[\ell_1(\kappa, \tau, \varphi | v, \mathbb{X}) + \ell_2(\alpha_k, \beta_k | v_k)]$$

where

$$\mathbb{E}[\ell_1(\kappa, \tau, \varphi | v, \mathbb{X})] = \sum_{i=1}^n \sum_{j=1}^{m_i} \mathbb{E} \left\{ -\frac{1}{2} \ln(2\pi |\Sigma \Delta t_{ij}|) - \frac{1}{2} (\Delta \mathbf{X}_{ij} - v \Delta t_{ij})' (\Sigma \Delta t_{ij})^{-1} (\Delta \mathbf{X}_{ij} - v \Delta t_{ij}) \right\} \quad (16)$$

and

$$\mathbb{E}[\ell_2(\alpha, \beta | v, X)] = \sum_{i=1}^n \sum_{j=1}^{m_i} \sum_{k=1}^d \left\{ \ln \alpha_k - \frac{1}{2} E[\ln(2\pi \beta_k v_k^3) | X] - E \left[\frac{(v_k - \alpha_k)^2}{2v_k \beta_k} | X \right] \right\} \quad (17)$$

For calculating $Q(\Theta | \Theta^{(l)})$ conditional \mathbb{X} and v , we use the Monte Carlo method with Metropolis-Hastings algorithm to sample the random effects v given the conditional pdf of v

$$\ln [f(v|X)] = -\frac{1}{2} \sum_{i=1}^n \sum_j^{m_i} \left\{ \ln(|\Sigma|) + (\Delta X_{ij} - v \Delta t_{ij})' (\Sigma \Delta t_{ij})^{-1} (\Delta X_{ij} - v \Delta t_{ij}) + \sum_{k=1}^d \left\{ \ln(v_k^3) + \frac{(v_k - \alpha_k)^2}{v_k \beta_k} \right\} \right\},$$

where the details of the Metropolis-Hastings and the MCEM algorithm are summarized in Supplementary S.2. Given the MCMC samples $\{v_k^{(l+1,b)}, b = 1, \dots, M, k = 1, \dots, d\}$, the value of $Q(\Theta|\Theta^{(l)})$ function can be calculated by averaging the log-likelihood values over all MCMC samples.

We can seek the maximum likelihood (ML) estimators for model parameters by maximizing the $Q(\Theta|\Theta^{(l)})$ function in the following M-step. By taking the first-order derivative of $\mathbb{E}[\ell_1(\kappa, \tau, \varphi|v, \mathbb{X})]$ in Equation 17 with respect to $\kappa^{(l+1)}$ and letting the derivative equal zero, we can update the estimate of $\kappa^{(l+1)}$ by

$$\kappa^{(l+1)} = \frac{1}{d \sum_{i=1}^n m_i} \sum_{i=1}^n \sum_{j=1}^{m_i} \sum_{k=1}^d E \left[\frac{(\Delta X_{ij}^{(k)} - v_k \Delta t_{ij})^2}{v_k \Delta t_{ij}} \right].$$

Similarly, the closed-form estimators for $\alpha_k^{(l+1)}$ and $\beta_k^{(l+1)}$ can be obtained by taking the first-order derivatives of $\mathbb{E}[\ell_{\neq}(\alpha, \beta|v, \mathbb{X})]$ in Equation 17 with respect to α_k and β_k and letting the derivatives equal zeros, which yields

$$\alpha_k^{(l+1)} = \frac{\sum_{i=1}^n \sum_{j=1}^{m_i} \sum_{k=1}^d E[v_k|\mathbb{X}]}{d \sum_{i=1}^n m_i},$$

$$\beta_k^{(l+1)} = \frac{d \sum_{i=1}^n m_i}{\sum_{i=1}^n \sum_{j=1}^{m_i} \sum_{k=1}^d \mathbb{E} \left[\frac{(v_k - \alpha_k^{(l+1)})^2}{v_k (\alpha_k^{(l+1)})^2} | \mathbb{X} \right]}.$$

Substituting $\alpha_k^{(l+1)}$, $\beta_k^{(l+1)}$, and $\kappa^{(l+1)}$ back into the expectation function $\mathbb{E}[\ell_1(\kappa, \tau, \varphi|v, \mathbb{X})]$ yields the profile log-likelihood function of τ and φ . The estimator of τ and φ in the $(l+1)$ th iteration can be readily obtained by numerically maximizing the profile log-likelihood. Repeat the E-step and M-step until the stopping criterion is satisfied.

The computational complexity of E-step in each iteration is $\mathcal{O}(N_0)$, $N_0 = Md \sum_{i=1}^n m_i$, since we compute the expectations by first averaging over M MCMC samples of the random drifts and then computing over $d \sum_{i=1}^n m_i$ observations of the degradation levels. The M-step at the l th iteration has closed-form expressions for the estimators $\kappa^{(l)}$, $\alpha_k^{(l)}$, and $\beta_k^{(l)}$ with computational complexity $\mathcal{O}(N_1)$, where $N_1 = d \sum_{i=1}^n m_i$. The M-step uses a numerical method to find the estimate $\tau^{(l)}$, where the computational complexity is the same as that in the EM algorithm in Section 3.2. Overall, the computational burden at each iteration of the MCEM algorithm is low.

5 Application analysis

In this section, two practical studies coming from the bearing degradation and the laser degradation are analyzed to illustrate the performance of the proposed model in degradation modeling and RUL prediction.

5.1 Practical study of the bearing degradation

The proposed multivariate degradation model in Equation 17 is applied to the degradation of bearings since the degradation data of bearings contain two-dimensional shock pulses with left-truncated observations.

5.1.1 Overview of the bearing degradation

As one of the critical elements of high-speed trains, bearings play an important role in reducing friction. Fatigue on the outer ring, which is the development and cumulation of cracks due to the material defect and rolling loadings, is the primary cause of bearing failures. The contact of the rolling elements with the defect area causes shock pulses which can reflect their degradation (Ahmad et al., 2017). To accurately predict the RUL of rolling bearings, shock pulse data are often used to understand the progress of fatigue development. As discussed in most literature (L. Wang et al., 2020), failure processes are often divided into more than one stage according to the defective state. The bearing failure process is generally divided into two stages, i.e. the first stage with healthy working conditions and the second stage with rapid degradation. The first stage lasts for a long duration in the life cycle of the bearing, with a slight shock pulse amplitude, thus providing limited information for the bearing degradation but burdening the data storage. Therefore, an economic observation strategy is to record the shock pulses from a used state based on empirical acknowledge. The resulting data are left-truncated degradation data with unknown truncation time.

There are over thousands of trains equipped with shock pulse measurement instruments. Sensors are installed in the bearing boxes to record daily shock pulses, as shown in Figure 4(a). Based on the resonance demodulation technic embedded in the operator, as shown in Figure 4(b), the dBn and dBsv are collected and used as two-dimensional performance characteristics. When any performance characteristic exceeds its predetermined threshold, the bearing is replaced. Figure 4(c,d) shows two of the run-to-failure rolling bearings, with severe peeling faults on the outer rings of the bearings.

5.1.2 RUL prediction of the bearing

To show the implementation of our method, we provide a step-by-step RUL prediction procedure for the bearing degradation application. Practitioners in other related fields with different appealing needs can establish the corresponding procedure similarly.

Step 1: degradation data pre-processing

The original shock pulses of the bearings over time are depicted in Figure 5, along with their features extracted by averaging the shock pulses every 250 km. As discussed in the introduction, the degradation paths in the same population vary from unit to unit due to the random effect. Moreover, the degradation data before an unknown running mileage τ are missing due to measurement instrument replacement. In this scenario, we cannot simply assume that the degradation data is complete. Since the fatigue of bearings is believed to follow the exponential law, we take the logarithm of the shock pulses. Besides, the shock pulses collected from the field using conditions are

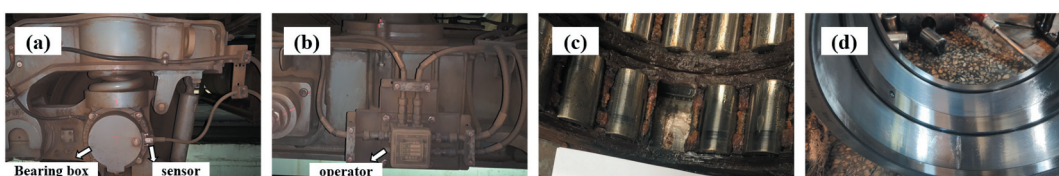


Figure 4. (A)-(b) Sensors and instruments used in data collection; (c)-(d) run-to-failure bearings.

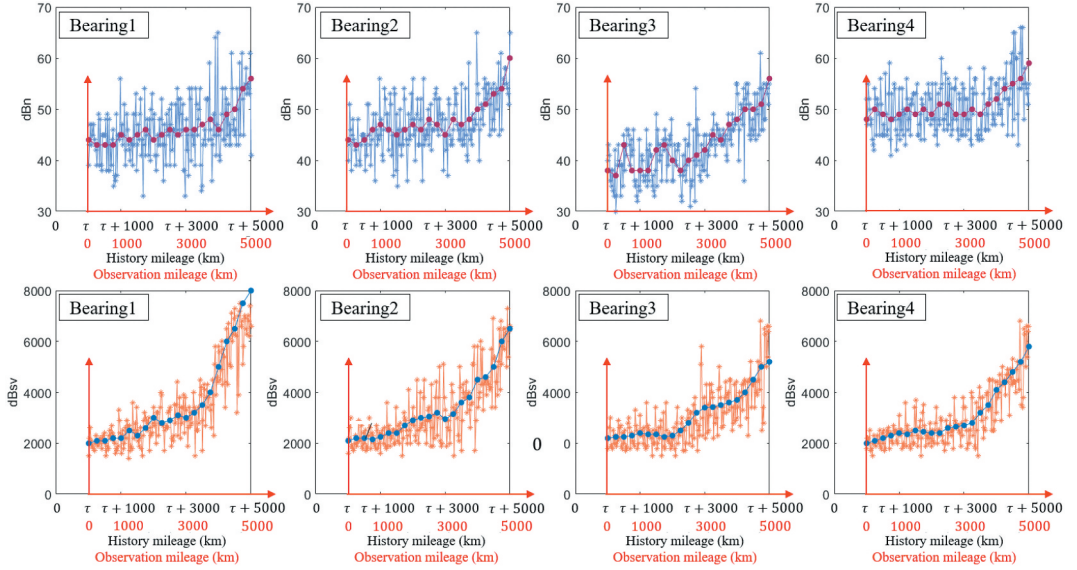


Figure 5. Original shock pulse data with left-truncated observations.

polluted by noises. Thus, a smooth operator is conducted by averaging every ten neighboring data points, and the results are used in the following degradation analysis.

Step 2: degradation model pre-analysis

Before applying the proposed model, we check whether the proposed model is appropriate for the bearing degradation data in terms of (i) the assumption of the positive correlation between the degradation rate and volatility and (ii) the assumption of the IG distribution $v\text{IG}(\alpha, \beta)$ for degradation rate v .

First, the correlation analysis between degradation rate and volatility is conducted based on the extracted degradation features in Figure 6. We fit each of the four bearings with a basic Wiener process, i.e. $X(t) = vt + \sigma B(t)$ and estimate their degradation drifts $\{\hat{v}_{ik}\}_{i=1}^4$ and diffusions $\{\hat{\sigma}_{ik}^2\}_{i=1}^4$, $k = 1, 2$. Here, \hat{v}_{ik} and $\hat{\sigma}_{ik}^2$ represent the estimates of the drift and diffusion of the k th PC from the i th bearing. We calculate the Pearson correlation coefficients by $\rho_k = \sum_{i=1}^n (\hat{v}_{ki} - \bar{v}_k)$

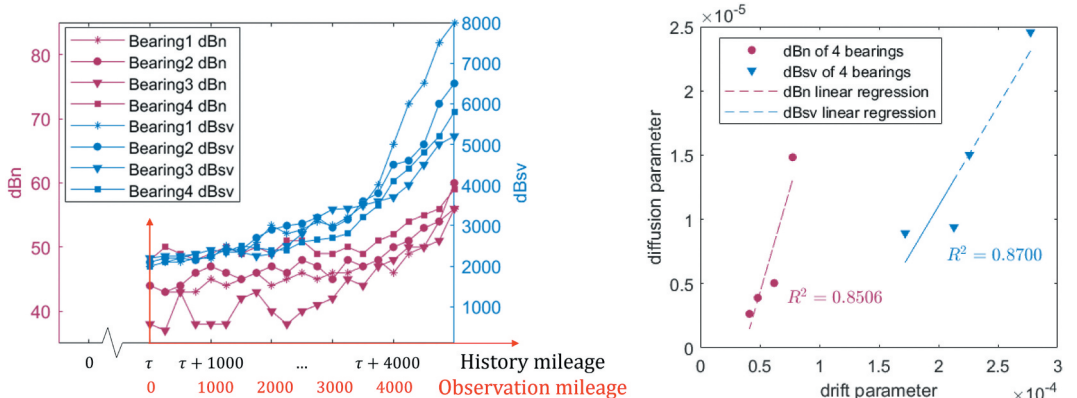


Figure 6. The degradation features from four bearings in the field using condition (left) and the correlation analysis between degradation rate and volatility (right).

$(\hat{\sigma}_{ki}^2 - \bar{\sigma}_k^2) / \sqrt{\sum_{i=1}^n (\hat{v}_{ki} - \bar{v}_k)^2} \sqrt{\sum_{i=1}^n (\hat{\sigma}_{ki}^2 - \bar{\sigma}_k^2)^2}$, $k = 1, 2$ to measure the linear correlation between degradation drifts $\{\hat{v}_{ik}\}_{i=1}^4$ and diffusions $\{\hat{\sigma}_{ik}^2\}_{i=1}^4$. Here, \bar{v}_k and $\bar{\sigma}_k^2$ are the sample means for $\{\hat{v}_{ik}\}_{i=1}^4$ and $\{\hat{\sigma}_{ik}^2\}_{i=1}^4$. Since correlation coefficients are $\rho_1 = 0.85$ and $\rho_2 = 0.87$, a strong positive correlation exists between the drift and diffusion parameters.

Second, we check that the IG distribution $v \mathcal{IG}(\alpha, \beta)$ is a judicious choice for the drift parameter v using the Kolmogorov-Smirnov (K-S) test and T-test. We compare the empirical cumulative distribution function (ECDF) of $\{\hat{v}_{ik}\}_{i=1}^4$ with the expected distribution $v_k \mathcal{IG}(\alpha_k, \beta_k)$, $k = 1, 2$. In other words, we conduct two distribution tests. For the first test, the null hypothesis is that $\{\hat{v}_{i1}\}_{i=1}^4$ from the first PC (i.e. the logarithm of dBn) follows an IG distribution. For the second test, the null hypothesis is that $\{\hat{v}_{i2}\}_{i=1}^4$ from the second PC (i.e. the logarithm of dBsv) follows an IG distribution. Regarding the K-S test, the p -values for the two tests are 0.9265 and 0.9542, respectively. In terms of the T-test, the p -values for the two tests are 0.9857 and 0.8374, respectively. Since the p -values are significantly greater than 0.05, there is no significant evidence to reject the IG distribution for the drift parameter.

Step 3: RUL prediction

We use the proposed model to analyze the bearing degradation data. A leave-one-out cross-validation is used. Specifically, we leave one bearing as a single-item test unit and fit the proposed model using all three other bearings. Given estimates of the model parameters, we predict the RUL for the test unit. Each bearing is selected as a test unit, and the total number of folds equals the number of bearings in our degradation data set. For each fold, the MCEM algorithm in Section 4.2 is used to estimate the model parameters iteratively. The algorithm converges within 50 iterations consuming around 110 s on a personal computer with AMD Ryzen 7(5800 H) 3.20 GHz processor. To ensure that the estimates converge to a steady state, we fix the number of iterations to 100.

To evaluate the performance of the proposed model in Equation 17, we compare it with three benchmarks. The first comparison model captures the degradation process by $X(t) = \varphi + vt + \Sigma^{1/2}B(t)$, $v_k \sim \mathcal{IG}(\alpha_{||}, \beta_{||})$. It neglects the truncation time and the jointly random effects of drift-diffusion. The second comparison model describes the degradation process by $X(t) = \varphi + vt + \Sigma^{1/2}B(t)$, $v_k \sim \mathcal{IG}(\alpha_{||}, \beta_{||})$, where $\Sigma^{1/2}$ has diagonal elements $\kappa^2 v_k$ and off-diagonal elements zeros. It only considers the jointly random effects of drift-diffusion and neglects the truncation time. The third comparison model only considers the truncation time by modeling the degradation process with $X(t) = \varphi + v(t + \tau) + \Sigma^{1/2}B(t + \tau)$, $v_k \sim \mathcal{IG}(\alpha_k, \beta_k)$, and it neglects the jointly random effects of drift-diffusion.

We fit the degradation data from four bearings for each candidate model and summarize the parameter estimates in Table 1. Since the parameter estimation methods for the three benchmarks are similar to the proposed model but simpler, we omit the details here. We also calculate the log-likelihood value for each model. The results show that the proposed model fits the degradation data best in terms of the log-likelihood value. The proposed model and the comparison model-3 consider the truncation time in their model assumptions. For both models, the non-zero estimates of left truncation time are consistent with our intuition that some degradation levels are missing before our observations start.

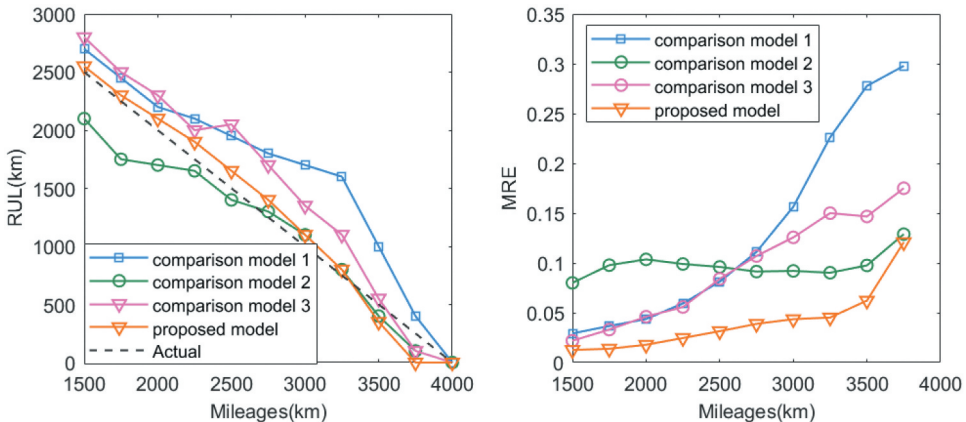
Due to the high dimensions of model parameters, the closed-form expression of RUL distribution is unavailable. The bootstrap method is used to predict the RUL. We simulate degradation paths with a large enough sample size according to the proposed model in Equation 17 given parameter estimates. Then, based on the re-generated degradation paths and the failure thresholds, we record the RUL for each degradation path. The expectation of the RUL can be obtained based on the simulated RULs. We evaluate the performance of the RUL predictions using mean absolute relative errors (MRE). The MRE is

Table 1. Parameter estimates of bearing degradation data.

Model	Parameter estimates	log-likelihood
Comparison model-1	$\varphi_1 = 3.77, a_1 = 0.57 \times 10^{-4}, \beta_1 = 9.7 \times 10^{-4}, \Sigma = \begin{bmatrix} 1.01 \times 10^{-6} & 0.11 \times 10^{-6} \\ 0.11 \times 10^{-6} & 4.02 \times 10^{-6} \end{bmatrix}$	72.6
Comparison model-2	$\varphi_1 = 3.77, a_1 = 6.23 \times 10^{-5}, \beta_1 = 2.45 \times 10^{-5}, \kappa = 0.1986$	139.3
Comparison model-3	$\varphi_1 = 1.57, \tau = 38636, a_1 = 0.57 \times 10^{-4}, \beta_1 = 9.7 \times 10^{-4}, \varphi_2 = -0.94, a_2 = 2.22 \times 10^{-4}, \beta_2 = 0.0076, \Sigma = \begin{bmatrix} 1.01 \times 10^{-6} & 1.11 \times 10^{-6} \\ 1.11 \times 10^{-6} & 4.02 \times 10^{-6} \end{bmatrix}$	88.5
Proposed Model	$\varphi_1 = 1.46, \tau = 40598, a_1 = 0.57 \times 10^{-4}, \beta_1 = 0.09, \varphi_2 = -1.78, a_2 = 2.32 \times 10^{-4}, \beta_2 = 0.11, \kappa = 0.1793$	172.2

computed by $MRE = \sum_{j=1}^m |\hat{l}_j - l_j| / (ml_j)$, where \hat{l}_j and l_j are the predicted and true values of the RUL at time t_j . The true RUL is known because all four bearings are run-to-failure by the end of our observations.

Results of RUL predictions from different models are shown in Figures 7–10. For bearings 2–4, as time goes on, the RUL predicted by the proposed model tends to be more adjacent to the true values than the other models. For bearing 1, during the entire degradation process, the proposed model shows more neighboring RUL predictions to the true RUL than the benchmark models. The MREs also indicate a better performance of the proposed model than the other models. The MREs of RUL prediction at the last prediction points are summarized in Table 2, which indicates a good accuracy of the proposed model in RUL prediction.

**Figure 7.** RUL prediction and prediction errors of bearing 1.**Table 2.** Mres for RUL predictions at the last time point.

	Bearing 1	Bearing 2	Bearing 3	Bearing 4
Comparison model-1	0.2979	0.2939	0.2367	0.2748
Comparison model-2	0.1289	0.1979	0.0995	0.2537
Comparison model-3	0.1750	0.1608	0.0995	0.2272
Proposed Model	0.1208	0.1207	0.0565	0.1964

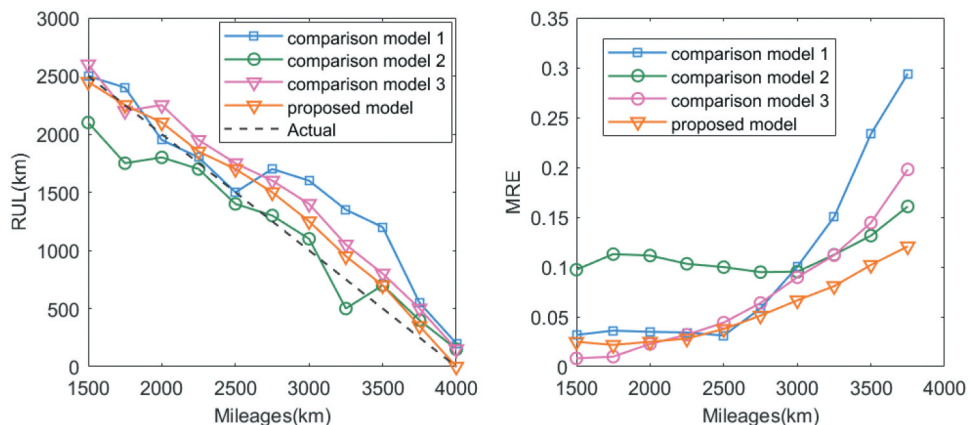


Figure 8. RUL prediction and prediction errors of bearing 2.

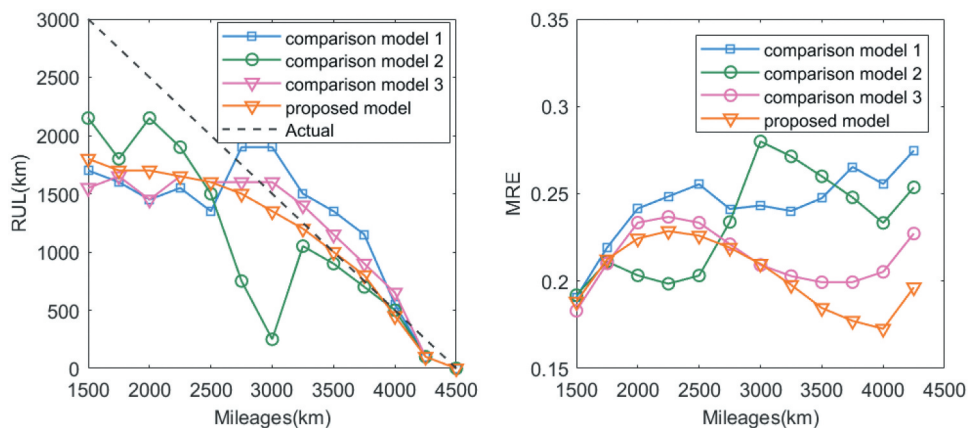


Figure 9. RUL prediction and prediction errors of bearing 3.

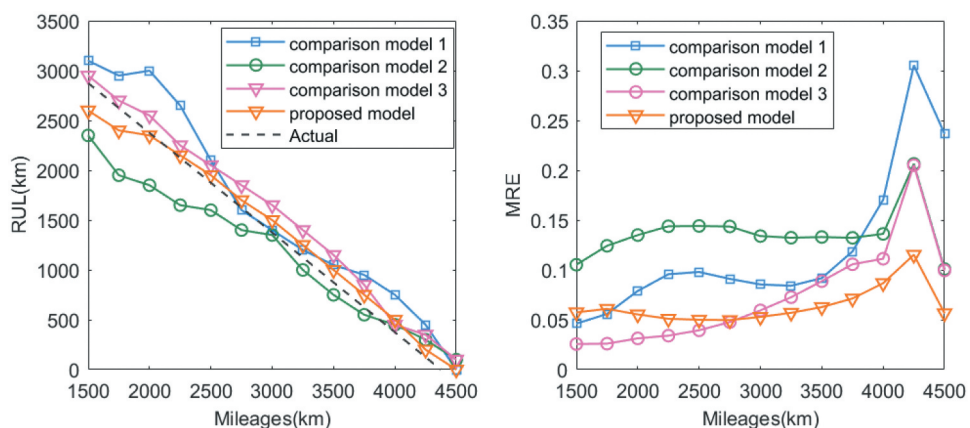


Figure 10. RUL prediction and prediction errors of bearing 4.

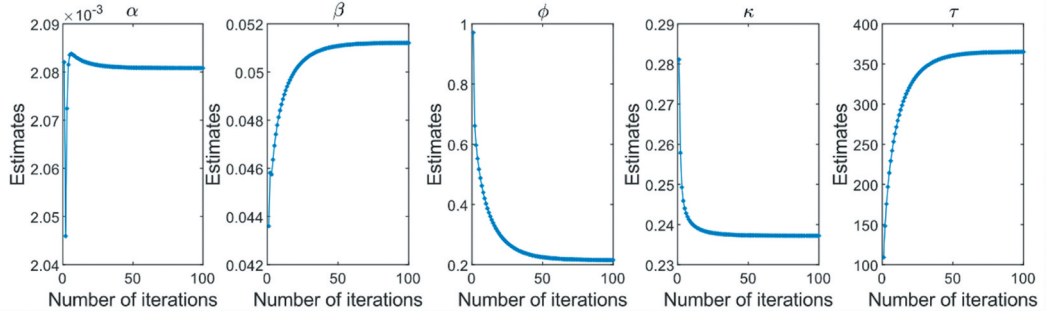


Figure 11. Number of iterations versus the estimates.

5.2 Practical study of the laser degradation

The Wiener process model used for bearing degradation data is developed for multivariate degradation. To illustrate cases with univariate degradation data, we employ the proposed model in Equation 1 to analyze the laser degradation data, with one performance characteristic degrading over time.

5.2.1 Overview of the laser degradation

The operating current is an important performance characteristic for GaAs lasers, whose value would increase with time and ultimately exceed a threshold, failing GaAs laser devices. Meeker et al (Meeker & Escobar, 2014) presented the percent increases in the operating current for 15 tested lasers. For illustration purposes, we assume that the degradation data before 500 hours are truncated. We use the observed data to perform the degradation modeling and RUL prediction. The failure threshold is set as $w = 6$. Before using the proposed model, we also check the rationality of the IG distribution drift

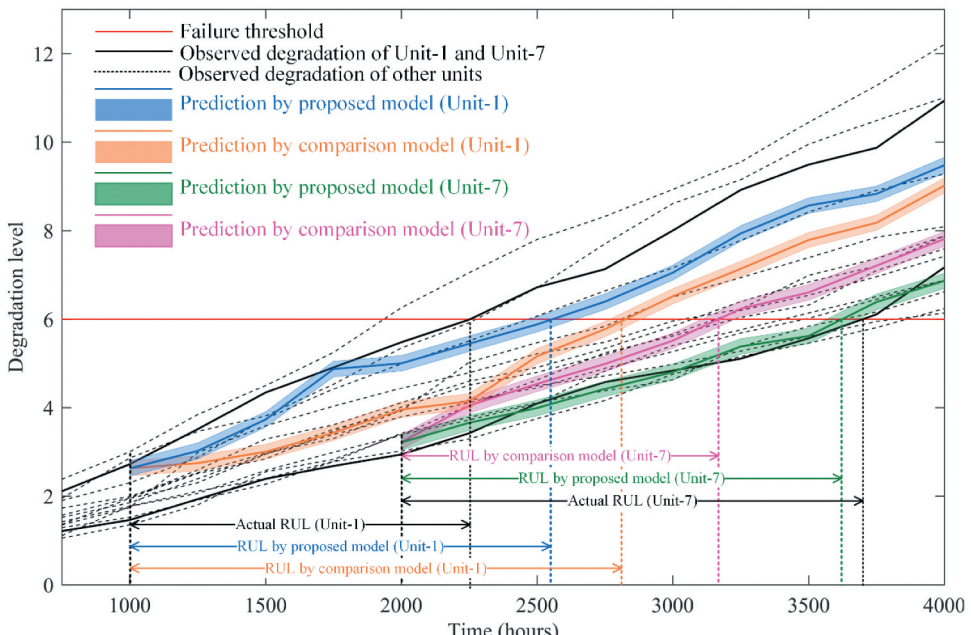


Figure 12. Degradation prediction for GaAs lasers at 1000 hours and 2000 hours.

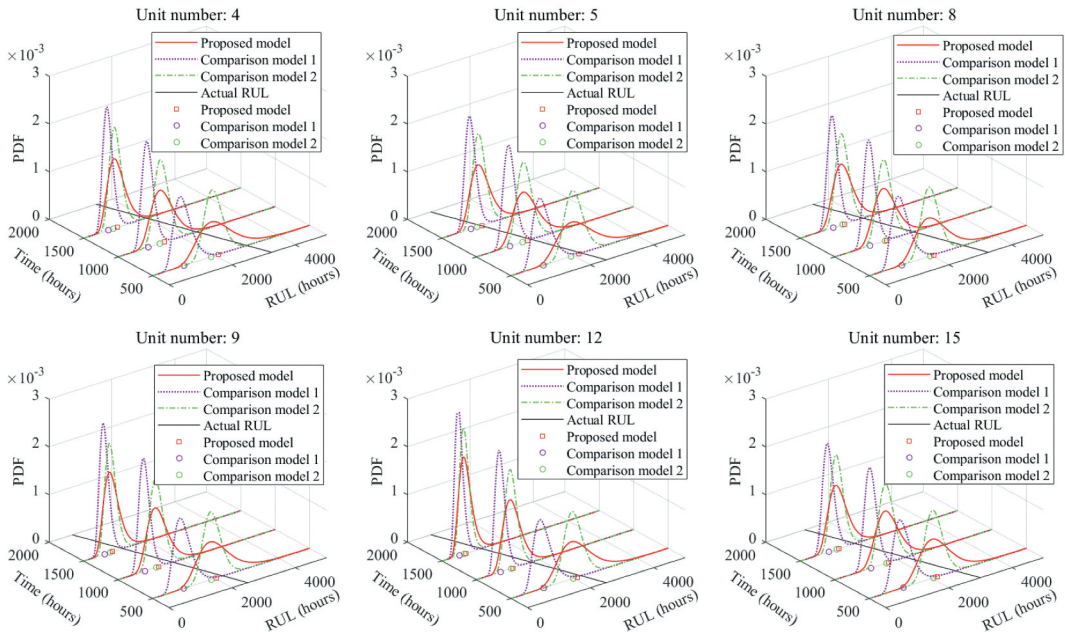


Figure 13. PDF of RUL for GaAs lasers.

parameter using the K-S and T-tests. The details of the test are similar to that in Section 5.1.2. Results show that the p -values of the K-S test and T-test are 0.9029 and 0.9568, respectively, indicating that the drift parameter follows the IG distribution at the 0.05 significance level.

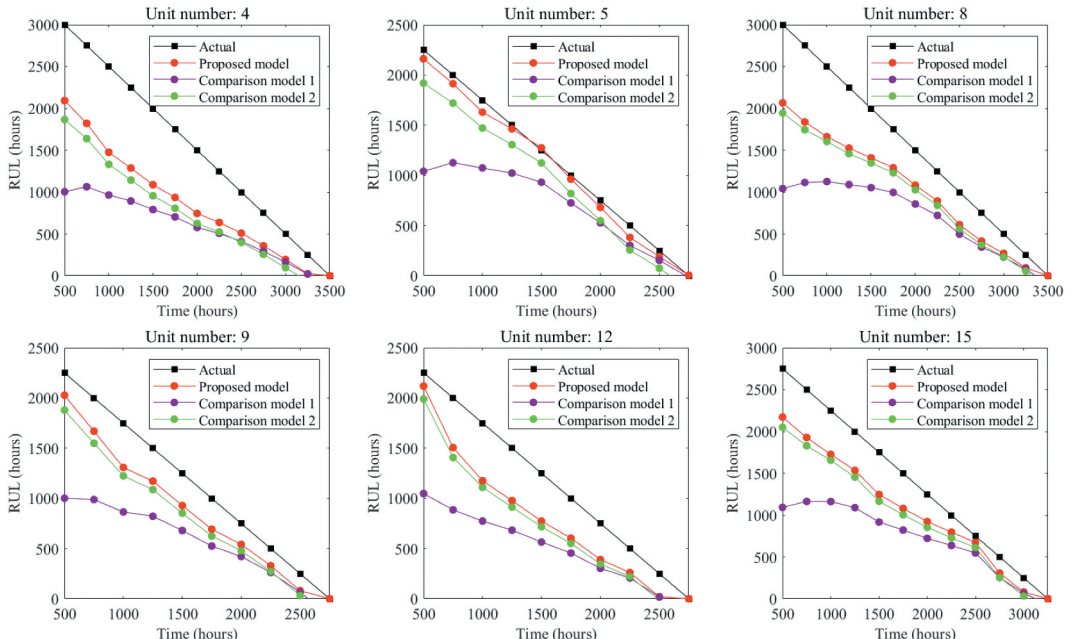


Figure 14. RUL predictions of GaAs lasers.

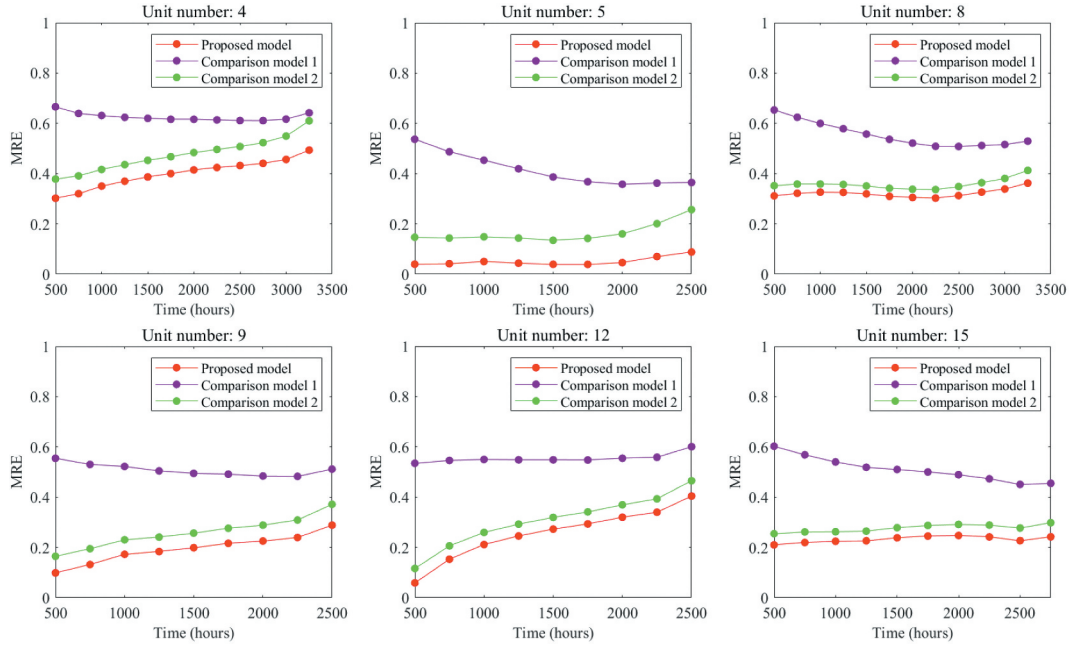


Figure 15. RUL prediction errors of GaAs lasers.

5.2.2 RUL prediction of the laser degradation

To show the implementation of our method in univariate degradation cases, we also provide a step-by-step RUL prediction procedure for the laser degradation data. Different from the degradation data analysis for bearing degradation in Section 5.2, we may not need the pre-processing procedure

Table 3. MRE for RUL predictions for GaAs lasers.

	Unit 1	Unit 2	Unit 3	Unit 4	Unit 5	Unit 6	Unit 7	Unit 8
Compared Model-1	0.5660	0.2839	0.4829	0.6416	0.3650	0.4776	0.4200	0.5291
Compared Model-2	0.3232	0.1322	0.3582	0.6097	0.2568	0.3438	0.2517	0.4128
Proposed Model	0.3411	0.1043	0.2780	0.4932	0.0881	0.2264	0.2110	0.3623
	Unit 9	Unit 10	Unit 11	Unit 12	Unit 13	Unit 14	Unit 15	
Compared Model-1	0.5113	0.5250	0.4408	0.6003	0.4576	0.4163	0.4550	
Compared Model-2	0.3712	0.1892	0.2833	0.4653	0.2900	0.2562	0.2986	
Proposed Model	0.2883	0.1284	0.1997	0.4040	0.2030	0.1662	0.2424	

for laser degradation data. This is because the degradation data from lasers come from the in-lab degradation test, where the working conditions are well controlled.

Step 1: parameter estimation

We use the proposed model to fit the laser degradation data with the EM algorithm in Section 3.2. The algorithm converges within 30 iterations consuming around 10 s. Similar to Section 5.1.2, we fix the number of iterations to 100 to ensure a steady state of convergence. As we have remarked in Section 3.2, one can also graphically check the convergence of the algorithm. As shown in Figure 11, the estimates of the model parameters converge to steady states. For practitioners eager to implement the EM algorithm, we provide the source code on GitHub, along with the laser degradation data (<https://github.com/Yan9564/TruncatedWiener>).

We make one remark on the performance of the EM algorithm. To evaluate the performance of the EM algorithm, we conduct additional simulation studies. We first set the model parameters and sample size in the degradation model in Equation 1 and then generate degradation data from the model. Then, we estimate the model parameters using the EM algorithm. The performance of the EM algorithm can be evaluated by comparing the estimates and the true parameters. This procedure is replicated 1000 times. The details of the simulation results are provided in Supplementary S.4 and Supplementary S.5.

Step 2: degradation prediction

We take unit-1 and unit-7 as examples to describe the procedure for degradation prediction. Leave-out cross-validation is conducted. Except for unit-1, degradation data from all the other units are used to estimate the model parameters. Given the parameter estimates, we predict the future degradation level for unit-1 from $t = 1000$ hours. The degradation levels for unit-7 from $t = 2000$ hours are predicted analogously. The interval of degradation predictions can be obtained by Monte-Carlo simulations. Specifically, we simulate the degradation levels for a large number of times (1000 times) given parameter estimates. The upper and lower confidence limits of the simulated degradation levels can be obtained by fitting the degradation levels to the normal distribution.

To evaluate the performance of the degradation prediction, we compare the proposed model with a benchmark. The comparison model describes the degradation data by $X(t) = \varphi + v(\tau + t) + \sigma\mathcal{B}(\tau + t)$, where both v and σ are constants. The comparison model neglects the joint random effects on degradation drift-diffusion. Figure 12 presents the degradation prediction results. The colored area plots the interval of degradation predictions with a 60% confidence level. Results indicate that the proposed model has a closer degradation path to the true degradation than the comparison model. Moreover, Figure 12 gives the RUL predictions at $t = 1000$ and $t = 2000$. The RUL predicted by the proposed model is closer to the actual RUL than the comparison model for both units. For unit-1, the failure time predicted by the comparison model is much later than the true failure time, leading to an overrating in the product's performance, which could result in safety risk in applications. For unit-7, the RUL predicted by the comparison model is much shorter than the actual RUL, which may lead to an inappropriate maintenance policy with additional cost.

Step 3: RUL prediction

To evaluate the performance of the proposed model in RUL prediction, we consider two benchmark models. The first comparison model overlooks the jointly random effects on the drift and diffusion parameters, which is the comparison model used in the second step. The second comparison model captures the degradation process by $X(t) = \varphi + vt + \sigma\mathcal{B}(t)$, which neglects the jointly random effects and the truncation time.

The dataset is used for RUL prediction by leave-one-out cross-validation. For illustration, distributions of the RULs at different times are presented in Figure 13. The PDF obtained from the proposed model has a squatter and fatter shape due to the statistical properties of the proposed model. This result is acceptable to the RUL prediction considering that the shape of PDF would be thinner over time. The discussion details are shown in Supplementary S.3. More importantly, for the proposed model, the point estimates of RUL at 500 h, 1000 h, and 1500 h are closer to the actual RUL than the comparison models.

We also predict the RUL for each of the 15 units using leave-one-out cross-validation. The prediction results and mean absolute relative errors (MRE) of the predictions are shown in Figures 14 and 15. Only six randomly selected units are presented here due to limited space, while prediction results for each of the 15 units are presented in Table 3. Overall, the results indicate that the proposed model performs better in RUL prediction than the comparison models. This consequence may be because the comparison models neglect the jointly random effects of drift-diffusion and left-truncated degradation. Table 3 shows the MRE of the RUL predictions from different models, which indicates the best performance of the proposed model among the candidate models.

6 Conclusions

Product degradation data are commonly collected from a non-brand-new state of the product, leading to the left-truncated degradation data. Such truncated degradation data introduces sample biases and complicates the degradation modeling. Traditional Wiener process models cannot describe this scenario due to the assumptions of complete degradation data. We propose a Wiener process model incorporating the truncation time to capture the degradation process more accurately. To describe the random effects, the proposed model incorporates an IG-distributed drift parameter to quantify the heterogeneities of degradation rate and degradation volatility by incorporating a nonlinear function between drift and diffusion parameters. Closed forms of parameter estimates and RUL distribution are derived with the help of the EM algorithm. We extended the proposed model to multivariate degradation analysis based on the same consideration, where model parameters can be estimated by incorporating MCMC sampling in the expectation step of the EM algorithm. Extensive simulation studies illustrated the performance of the EM algorithm and RUL prediction method. Implementation procedures are illustrated step-by-step with two real applications. The results of these applications demonstrate that the proposed model can deal well with the left-truncated degradation data and jointly random effects of drift-diffusion in RUL prediction.

The current study has three possible extensions for future works. First, the truncation time in a population is assumed as a constant in this paper, while the observations for different units may start from different times. We can consider the random effect of the truncation time based on the current work. Second, the impact of the measurement error on degradation observations is worth investigating. However, the measurement error may increase the complexity of computation. Thereby, an efficient statistical inference method should be proposed for the model. Third, the random effect of degradation drift is assumed to be IG distributed in this paper. Other candidate distributions might be more appropriate and general in the actual application, i.e. log-normal distribution, truncated-normal distribution, and general inverse Gaussian distribution.

Disclosure statement

No potential conflict of interest was reported by the authors.

Funding

The work was supported by the National Natural Science Foundation of China [72201019]; Reliability and Environmental Engineering Science & Technology Laboratory [6142004210105]; National Natural Science Foundation of China [52075020]; China Scholarship Council [202106020153]

Notes on contributors

Bingxin Yan received her B.S. degree in 2018 from Beihang University. She is currently a Ph.D. candidate at School of Reliability and Systems Engineering, Beihang University. Her research interests include industrial statistics and remaining useful life prediction.

Han Wang received a Ph.D. degree in systems engineering from Beihang University, Beijing, P.R. China, in 2020. He is currently a postdoctoral researcher with the School of Aeronautic Science and Engineering, Beihang University. His research interests include accelerated tests, stochastic degradation modelling, and fault prognosis.

Xiaobing Ma received a Ph.D. degree in engineering mechanics from Beihang University, Beijing, P.R. China, in 2006. He is currently a Professor with the School of Reliability and Systems Engineering, Beihang University. His current research interests include reliability data analysis, durability design, and system life modelling.

ORCID

Xiaobing Ma  <http://orcid.org/0000-0002-0913-9012>

References

- Ahmad, W., Khan, S. A., & Kim, J. M. (2017). A hybrid prognostics technique for rolling element bearings using adaptive predictive models. *IEEE Transactions on Industrial Electronics*, 65(2), 1577–1584. <https://doi.org/10.1109/TIE.2017.2733487>
- Bian, L., & Gebraeel, N. (2014b). Stochastic modeling and real-time prognostics for multi-component systems with degradation rate interactions. *IIE Transactions: Industrial Engineering Research & Development*, 46(5), 470–482. <https://doi.org/10.1080/0740817X.2013.812269>
- Bian, L., Gebraeel, N., & Kharoufeh, J. P. (2015). Degradation modeling for real-time estimation of residual lifetimes in dynamic environments. *IIE Transactions*, 47(5), 471–486. <https://doi.org/10.1080/0740817X.2014.955153>
- De Santis, R. B., Gontijo, T. S., & Costa, M. A. (2022). Condition-based maintenance in hydroelectric plants: A systematic literature review. *Proceeding ImechE, Part O: J Risk and Reliability*, 236(5), 631–646. doi: <https://doi.org/10.1177/1748006X211035623>
- Giorgio, M., Postiglione, F., & Pulcini, G. (2020). Bayesian estimation and prediction for the transformed Wiener degradation process. *Appl Stoch Models in Bus Ind*, 36(4), 660–678. <https://doi.org/10.1002/asmb.2522>
- Huynh, K. T. (2019). A hybrid condition-based maintenance model for deteriorating systems subject to nonmemoryless imperfect repairs and perfect replacements. *IEEE Transactions on Reliability*, 69(2), 781–815. <https://doi.org/10.1109/TR.2019.2942019>
- Isciglu, F., & Erem, A. (2021). Reliability analysis of a multi-state system with identical units having two dependent components. *Proceedings of the Institution of Mechanical Engineers, Part O: Journal of Risk and Reliability*, 235(2), 241–252. <https://doi.org/10.1177/1748006X20957476>
- Jiang, W., Ye, Z. S., & Zhao, X. (2020). Reliability estimation from left-truncated and right-censored data using splines. *Statistica Sinica*, 30(2), 845–875.
- Lee, M. Y., Hu, C. H., & Tang, J. (2017). A two-stage latent variable estimation procedure for time-censored accelerated degradation tests. *IEEE Transactions on Reliability*, 66(4), 1266–1279. <https://doi.org/10.1109/TR.2017.2731680>
- Lee, J., Ni, J., Singh, J., Jiang, B., Azamfar, M., & Feng, J. (2020). Intelligent maintenance systems and predictive manufacturing. *Journal of Manufacturing Science and Engineering*, 142(11), 110805. <https://doi.org/10.1115/1.4047856>
- Li, N., Lei, Y., Yan, T., Li, N., & Han, T. (2018). A Wiener-process-model-based method for remaining useful life prediction considering unit-to-unit variability. *IEEE Transactions on Industrial Electronics*, 66(3), 2092–2101. <https://doi.org/10.1109/TIE.2018.2838078>
- Limon, S., Rezaei, E., & Yadav, O. P. (2020). Designing an accelerated degradation test plan considering the gamma degradation process with multi-stress factors and interaction effects. *Quality Technology & Quantitative Management*, 17(5), 544–560. <https://doi.org/10.1080/16843703.2019.1696010>
- Liu, X., Al-Khalifa, K. N., Elsayed, E. A., Coit, D. W., & Hamouda, A. S. (2014). Criticality measures for components with multi-dimensional degradation. *IIE Transactions*, 46(10), 987–998. <https://doi.org/10.1080/0740817X.2013.851433>
- Liu, S. W., Wu, C. W., & Wang, Z. H. (2022). An integrated operating mechanism for lot sentencing based on process yield. *Quality Technology & Quantitative Management*, 19(2), 139–152. <https://doi.org/10.1080/16843703.2021.1927295>
- Lu, L., Wang, B., Hong, Y., Ye Z. (2020). General path models for degradation data with multiple characteristics and covariates. *Technometrics*, 62(2), 1–16. <https://doi.org/10.1080/00401706.2020.1744909>
- Ma, Z., Wang, S., Liao, H., & Zhang, C. (2019). Engineering-driven performance degradation analysis of hydraulic piston pump based on the inverse Gaussian process. *Quality and Reliability Engineering International*, 35(7), 2278–2296. <https://doi.org/10.1002/qre.2502>
- Meeker, W. Q., & Escobar, L. A. (2014). *Statistical methods for reliability data*. John Wiley & Sons.
- Neumann, T., Dutschk, B., & Schenkendorf, R. (2019). Analyzing uncertainties in model response using the point estimate method: Applications from railway asset management. *Proceedings of the Institution of Mechanical Engineers, Part O: Journal of Risk and Reliability*, 233(5), 761–774. <https://doi.org/10.1177/1748006X19825593>
- Paroissin, C. (2015). Inference for the Wiener process with random initiation time. *IEEE Transactions on Reliability*, 65(1), 147–157. <https://doi.org/10.1109/TR.2015.2456056>
- Peng, C. Y., & Tseng, S. T. (2010). Progressive-stress accelerated degradation test for highly-reliable products. *IEEE Transactions on Reliability*, 59(1), 30–37. <https://doi.org/10.1109/TR.2010.2040769>
- Peng, R., Wu, D., Xiao, H., Xing, L., & Gao, K. (2019). Redundancy versus protection for a non-reparable phased-mission system subject to external impacts. *Reliability Engineering & System Safety*, 191, 106556. <https://doi.org/10.1016/j.ress.2019.106556>
- Shahraki, A. F., Yadav, O. P., & Liao, H. (2017). A review on degradation modelling and its engineering applications. *International Journal of Performability Engineering*, 13(3), 299. <https://doi.org/10.23940/ijpe.17.03.p6.299314>

- Shen, L., Wang, Y., Zhai, Q., & Tang, Y. (2018). Degradation modeling using stochastic processes with random initial degradation. *IEEE Transactions on Reliability*, 68(4), 1320–1329. <https://doi.org/10.1109/TR.2018.2885133>
- Singleton, R. K., Strangas, E. G., & Aviyente, S. (2016). The use of bearing currents and vibrations in lifetime estimation of bearings. *IEEE Transactions on Industrial Informatics*, 13(3), 1301–1309. <https://doi.org/10.1109/TII.2016.2643693>
- Su, C., Li, L., & Wen, Z. (2020). Remaining useful life prediction via a variational autoencoder and a time-window-based sequence neural network. *Quality and Reliability Engineering International*, 36(5), 1639–1656. <https://doi.org/10.1002/qre.2651>
- Sun, Q., Ye, Z. S., & Hong, Y. (2020). Statistical modeling of multivariate destructive degradation tests with blocking. *Technometrics*, 62(4), 536–548. <https://doi.org/10.1080/00401706.2019.1668855>
- Tsai, C. C., Tseng, S. T., & Balakrishnan, N. (2011). Mis-specification analyses of gamma and Wiener degradation processes. *Journal of Statistical Planning and Inference*, 141(12), 3725–3735. <https://doi.org/10.1016/j.jspi.2011.06.008>
- Wang, F. K., & Mamo, T. (2019). Hybrid approach for remaining useful life prediction of ball bearings. *Quality and Reliability Engineering International*, 35(7), 2494–2505. <https://doi.org/10.1002/qre.2538>
- Wang, D., & Tsui, K. L. (2018). Brownian motion with adaptive drift for remaining useful life prediction: Revisited. *Mechanical Systems and Signal Processing*, 99, 691–701. <https://doi.org/10.1016/j.ymssp.2017.07.015>
- Wang, X., Wang, B. X., Wu, W., & Hong, Y. (2020). Reliability analysis for accelerated degradation data based on the Wiener process with random effects. *Quality and Reliability Engineering International*, 36(6), 1969–1981. <https://doi.org/10.1002/qre.2668>
- Wang, L., Yang, Y., Zhu, H., & Liu, G. (2020). Optimal condition-based renewable warranty policy for products with three-stage failure process. *Quality Technology & Quantitative Management*, 17(2), 216–233. <https://doi.org/10.1080/16843703.2019.1584956>
- Wang, Z., Zhai, Q., & Chen, P. (2021). Degradation modeling considering unit-to-unit heterogeneity-A general model and comparative study. *Reliability Engineering and System Safety*, 216, 107897. <https://doi.org/10.1016/j.ress.2021.107897>
- Weaver, B. P., Meeker, W. Q., Escobar, L. A., & Wendelberger J. (2013). Methods for planning repeated measures degradation studies. *Technometrics*, 55(2), 122–134. <https://doi.org/10.1080/00401706.2012.715838>
- Wu, C. W., Shu, M. H., & Wu, N. Y. (2021). Acceptance sampling schemes for two-parameter Lindley lifetime products under a truncated life test. *Quality Technology & Quantitative Management*, 18(3), 382–395. <https://doi.org/10.1080/16843703.2020.1846269>
- Xiao, X., & Ye, Z. S. (2016). Optimal design for destructive degradation tests with random initial degradation values using the Wiener process. *IEEE Transactions on Reliability*, 65(3), 1327–1342. <https://doi.org/10.1109/TR.2016.2575442>
- Ye, Z. S., Chen, N., & Shen, Y. (2015). A new class of Wiener process models for degradation analysis. *Reliability Engineering & System Safety*, 139, 58–67. <https://doi.org/10.1016/j.ress.2015.02.005>
- Ye, Z. S., & Xie, M. (2015). Stochastic modelling and analysis of degradation for highly reliable products. *Applied Stochastic Models in Business and Industry*, 31(1), 16–32. <https://doi.org/10.1002/asmb.2063>
- Yuan, X. X., & Pandey, M. D. (2009). A nonlinear mixed-effects model for degradation data obtained from in-service inspections. *Reliability Engineering & System Safety*, 94(2), 509–519. <https://doi.org/10.1016/j.ress.2008.06.013>
- Zhai, Q., Chen, P., Hong, L., & Shen, L. (2018). A random-effects Wiener degradation model based on accelerated failure time. *Reliability Engineering & System Safety*, 180, 94–103. <https://doi.org/10.1016/j.ress.2018.07.003>
- Zhang, Y. (2022). Stochastic comparisons of conditional residual lifetimes with applications. *Quality Technology & Quantitative Management*, 1–32. <https://doi.org/10.1080/16843703.2022.2136281>
- Zhang, J. X., Hu, C. H., Si, X. S., Zhou, Z. -J., & Du, D. -B. (2014). Remaining useful life estimation for systems with time-varying mean and variance of degradation processes. *Quality and Reliability Engineering International*, 30(6), 829–841. <https://doi.org/10.1002/qre.1705>
- Zhang, Y., & Liao, H. (2014). Analysis of destructive degradation tests for a product with random degradation initiation time. *IEEE Transactions on Reliability*, 64(1), 516–527. <https://doi.org/10.1109/TR.2014.2336411>
- Zhang, Z., Si, X., Hu, C. H., & Lei, Y. (2018). Degradation data analysis and remaining useful life estimation: A review on Wiener-process-based methods. *European Journal of Operational Research*, 271(3), 775–796. <https://doi.org/10.1016/j.ejor.2018.02.033>
- Zhao, X., Huang, X., & Sun, J. (2020). Reliability modeling and maintenance optimization for the two-unit system with preset self-repairing mechanism. *Proceedings of the Institution of Mechanical Engineers, Part O: Journal of Risk and Reliability*, 234(2), 221–234. <https://doi.org/10.1177/1748006X19890739>
- Zhou, R., Gebraeel, N., & Serban, N. (2012). Degradation modeling and monitoring of truncated degradation signals. *IIE Transactions: Industrial Engineering Research & Development*, 44(9), 793–803. <https://doi.org/10.1080/0740817X.2011.618175>
- Zhou, S., Tang, Y., & Xu, A. (2021). A generalized Wiener process with dependent degradation rate and volatility and time-varying mean-to-variance ratio. *Reliability Engineering and System Safety*, 216, 107895. <https://doi.org/10.1016/j.ress.2021.107895>